Fuel-Cell-Grade H_2 from Hydrocarbons

Catalytic Reforming of Oxygenated Hydrocarbons for Hydrogen with Low Levels of Carbon Monoxide**

*Rupali R. Davda and James A. Dumesic**

The production of fuel-cell-grade hydrogen, containing very low levels of CO, is critical for the global transition to a hydrogen society. In spite of ongoing efforts to make fuel cells more CO-tolerant,[1] the use of hydrogen fuel-cells in portable applications (e.g., automobiles, battery replacement devices) is particularly challenging, as the production of hydrogen by steam-reforming of hydrocarbons[2] requires a complex combination of multiple processes[3–7] to achieve the required low CO levels (e.g., 100–500 ppm).[1] An important step toward a simple process for the production of hydrogen containing low levels of CO is made possible by the discovery[8] that hydrogen can be produced by catalytic reforming of biomass-derived oxygenated hydrocarbons in liquid water at temperatures near 500 K. This process has the advantage that the reforming of oxygenated hydrocarbons and the water–gas shift (WGS) reaction are both thermodynamically favorable at the same low temperatures, thus making it possible to conduct both reactions in one reactor. These low levels of CO, combined with the fact that our low-temperature process uses biomass-derived renewable feedstocks, makes aqueous-phase reforming of oxygenates an attractive process for applications in portable devices.

Herein, we show results from studies of the aqueous-phase reforming of ethylene glycol (EG) to produce H_2, with specific emphasis on the levels of CO produced as a function of the process conditions. We show the importance of the reaction operating conditions for achieving low levels of CO in the effluent gas from our single-reactor reforming process, and we elucidate the factors that control the ultimate levels of CO that can be attained.

Aqueous-phase reforming of oxygenates to produce H_2 takes place on metal catalysts[9] through C–C cleavage to make CO and H_2, [Eq. (1)].

$$C_2H_6O_2 \rightleftharpoons 2\,CO + 3\,H_2 \tag{1}$$

(Undesired alkanes are formed through C–O cleavage.) Adsorbed CO undergoes WGS [Eq. (2)], which increases the

$$CO + H_2O \rightleftharpoons CO_2 + H_2 \tag{2}$$

amount of H_2 produced and removes CO from the catalyst surface.[10]

The lowest partial pressure of CO that can be achieved depends on the thermodynamics of the WGS reaction and the operating conditions, [Eq. (3)].

$$P_{CO} = \frac{P_{CO_2} P_{H_2}}{K_{WGS} P_{H_2O}} \tag{3}$$

K_{WGS} is the equilibrium constant for the vapor-phase WGS and P_j are partial pressures. Since H_2, CO_2, and small amounts of alkanes (primarily CH_4) are produced by aqueous-phase reforming,[8] gas bubbles are formed within the liquid-phase flow reactor. The pressure in these bubbles can be approximated to be equal to the system pressure, [Eq. (4)].

$$P_{bubble} \approx P_{system} = P_{H_2O} + \sum_{products} P_j \tag{4}$$

The partial pressures of the reaction products and water vapor are dictated by the feed concentrations, system pressure and temperature, as outlined below.

For dilute product concentrations and system pressures above the saturation pressure of water, the bubbles contain water vapor at a pressure equal to its saturation pressure at the reactor temperature, and the remaining pressure is the sum of the partial pressures of the product gases. The extent of vaporization, y, is defined as the percent of water in the vapor phase relative to the total amount of water flowing into the reactor. In contrast, for systems operated at pressures that are near the saturation pressure of water, all the liquid water

[*] Prof. Dr. J. A. Dumesic, R. R. Davda
Chemical Engineering Department
University of Wisconsin
Madison, WI 53706 (USA)
Fax: (+1) 608-262-5434
E-mail: dumesic@engr.wisc.edu

[**] This work was supported by U.S. Department of Energy (DOE), Office of Basic Energy Sciences, Chemical Sciences Division. We thank Sibongile Nkosi and Jonathon Tomshine for help in collecting reaction kinetics data.

Supporting information for this article is available on the WWW under http://www.angewandte.org or from the author.

  DOI: 10.1002/ange.200351664

may vaporize, and the composition of the bubble is dictated by the stoichiometry of the feed stream. At this condition, the partial pressure of water is below its saturation pressure because the water vapor is diluted by the reforming product gases. Higher concentrations of EG lead to lower partial pressures of water because of greater dilution from H_2 and CO_2 produced by reforming reactions. As the system pressure is increased, the partial pressure of water vapor increases until it reaches the saturation pressure of water, at which point any further increase in the system pressure leads to partial condensation of water.

The above arguments indicate that the conditions which favor the lowest levels of CO from reforming of oxygenates are those which lead to the lowest partial pressures of H_2 and CO_2 in the reforming gas bubbles; and, these conditions are achieved by operating at system pressures that are near the saturation pressure of water and at low EG feed concentrations. As the system pressure increases and the extent of vaporization decreases below 100%, the partial pressures of H_2 and CO_2 in the bubble increase, thereby leading to higher equilibrium concentrations of CO. Similarly, as the EG concentration in the feed increases, higher partial pressures of H_2 and CO_2 are developed, even for the case of complete vaporization, again leading to higher equilibrium CO concentrations. This dependence of the CO concentration on the operating conditions for EG reforming has been corroborated with detailed experiments, as outlined below.

Table 1 summarizes results for aqueous-phase reforming of EG at feed concentrations of 2 wt% (runs 1–7), 5 wt% (runs 8–13) and 10 wt% (run 14). The upflow reactor (1.27 cm (0.5 inch) stainless-steel tube) containing the Pt/Al_2O_3 catalyst was divided into two separately heated reaction zones. Reforming reactions were carried out in the lower section (denoted as the reforming zone), maintained at 498 K (see Supporting Information for further details). The temperature of the top section (denoted as the shift zone), system pressure, feed concentration, and feed flow rate were varied in the different runs listed in Table 1. The weight hourly space velocity (WHSV) of EG, defined as the grams of EG per gram of catalyst per hour, was maintained such that complete conversion to gas phase products was achieved for all runs. The performance of the catalyst was stable for long periods of time on stream (e.g., 2 weeks). Results from replicate runs agreed to within $\pm 10\%$.

The data in Table 1 show that the dry effluent gas stream (after condensation of water) for each reaction condition consists primarily of H_2 and CO_2. The CO concentration in the effluent gas and the corresponding equilibrium concentration are reported for each condition. For the 2% and 5% EG feeds, detailed studies were conducted for system pressures of 25.8, 32.0 and 36.2 bar, with the shift zone of the reactor controlled at various temperatures. For the 10% feed, data were collected at 25.8 bar with the shift zone at 498 K. Higher system pressures lead to lower reaction rates,[11] resulting in a slightly lower conversion of the 10% EG feed.

As the saturation pressure of water at 498 K is equal to 25.1 bar, liquid water is completely vaporized at a system pressure of 25.8 bar. For 2% EG at this pressure (run 1), the H_2 pressure in the bubble is calculated to be 0.77 bar, and this condition leads to a low equilibrium CO concentration of 66 ppm in the reactor effluent. At system pressures of 32 and 36.2 bar (runs 2 and 3, respectively), the H_2 pressures are 4.60 and 7.53 bar, respectively, with only 18 and 11% vaporization of water occurring in each case. These conditions lead to higher equilibrium CO concentrations of 380 and 617 ppm, respectively. For the 5% EG feed at a system pressure of 25.8 bar (run 8), complete vaporization leads to a H_2 partial pressure of 1.79 bar, which results in a higher equilibrium CO concentration (163 ppm) compared to run 1 for the 2% feed. The effect of increasing system pressure for the 5% feed is similar to the behavior of 2% EG, as presented in runs 9 and 10 of Table 1.

The effect of H_2 pressure on the equilibrium CO concentration is illustrated in Figure 1a and 1b for the 2 and 5% feeds, respectively. It can be seen that the observed concentrations of CO are slightly lower than the calculated equilibrium values, especially for experiments conducted at higher system pressures. These lower values of CO concentrations are not caused by consumption of CO through methanation reactions. In particular, we conducted experi-

Table 1: Results for ethylene glycol (EG) reforming over 3% Pt/γ-Al_2O_3.

Run Number	1	2	3	4	5	6	7	8	9	10	11	12	13	14
EG Feed Concentration [wt%]	2	2	2	2	2	2	2	5	5	5	5	5	5	10
WHSV [g/gcat/hr]	0.0054	0.0054	0.0054	0.0054	0.0054	0.0027	0.0081	0.0135	0.0135	0.0135	0.0135	0.0135	0.0054	0.0270
Shift Temperature, T_s [K]	498	498	498	508	515	498	498	498	498	498	505	512	498	498
System Pressure [bar]	25.8	32.0	36.2	32.0	36.2	32.0	32.0	25.8	32.0	36.5	32.0	36.2	32.0	25.8
% Vaporization of Water, γ	100	18	11	91	90	16	16	100	41	22	100	100	42	100
H_2 Pressure in Vapor Phase [bar]	0.77	4.60	7.53	1.05	1.14	4.51	4.66	1.79	4.62	7.87	2.20	2.33	4.63	3.40
H_2O Pressure in Vapor Phase [bar]	24.4	25.1	25.1	30.1	34.1	25.1	25.1	22.6	25.1	25.1	28.5	32.4	25.1	20.7
H_2 [mol%]	69.8	69.6	70.0	69.1	68.9	68.3	70.4	69.9	69.7	70.9	69.3	69.0	70.0	69.6
CO_2 [mol%]	28.7	28.7	28.6	28.9	28.8	29.3	28.4	28.5	28.9	28.3	29.1	29.0	28.3	28.9
CH_4 [mol%]	1.38	1.43	1.06	1.64	2.02	1.66	0.99	1.35	1.09	0.51	1.34	1.70	1.37	1.34
C_2H_6 [mol%]	0.16	0.25	0.32	0.28	0.36	0.32	0.23	0.20	0.26	0.27	0.27	0.35	0.28	0.14
Experimental CO [ppm]	**60**	**326**	**564**	**84**	**89**	**363**	**328**	**118**	**305**	**558**	**163**	**183**	**341**	**196**
Equilibrium CO [ppm]	**66**	**380**	**617**	**88**	**95**	**380**	**379**	**163**	**382**	**638**	**185**	**195**	**377**	**341**

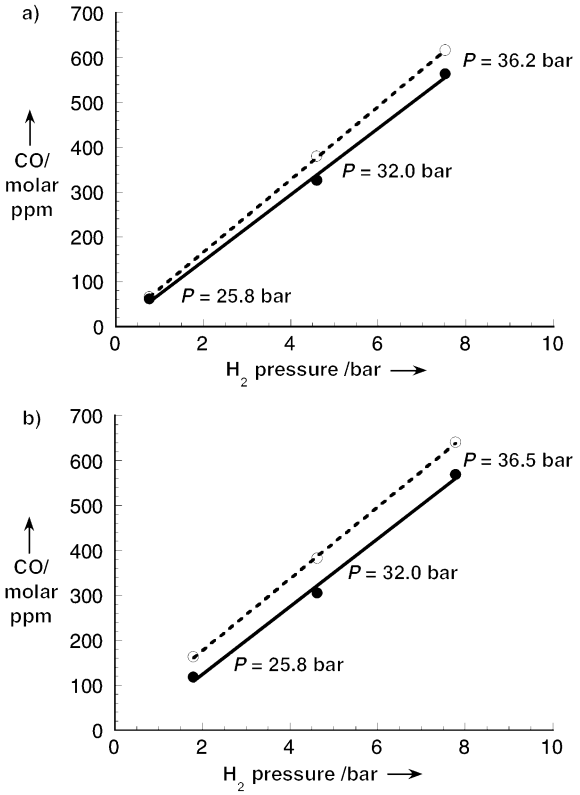

Figure 1. Effect of H_2 pressure on CO concentration for a) 2% EG (WHSV = 0.0054 h^{-1}) and b) 5% EG (WHSV = 0.0135 h^{-1}). Each point corresponds to a shift temperature of 498 K. Open symbols represent equilibrium CO and filled symbols represent observed CO.

ments in which water was co-fed with a simulated reformer gas (containing 1000 ppm CO in a 30:70 CO_2:H_2 mixture) over the Pt/Al_2O_3 catalyst at 498 K and a system pressure of 25.8 bar, such that the partial pressures of water and H_2 in the reactor were 21.6 and 2.95 bar, respectively (conditions similar to run 14). Under these conditions, we did not detect any measurable amounts of CH_4 and the concentration of CO in this simulated reformer gas was converted to the WGS equilibrium value of 298 ppm.

Our previous studies of EG reforming over Pt/Al_2O_3[11] have shown that reaction rates are lower at higher system pressures. Hence, we suggest that lower values of observed CO concentrations (compared to equilibrium values) at higher system pressures are caused by lower WGS rates. Accordingly, we conducted experiments to study the effect of WHSV on the deviations of the effluent CO concentrations from the equilibrium values. The WHSV was altered for 2 and 5% feeds at 32 bar (runs 6–7 and run 13) by changing the feed flow rate through the reactor. Also, for a particular volumetric flow rate, the WHSV is different for the three feed concentrations. Figure 2 shows the deviation of the observed CO concentration from the equilibrium value (expressed as a percentage of the equilibrium value) as a function of WHSV for runs conducted at 498 K. Higher temperatures (runs 4, 5, 11 and 12) were not included in this plot, because the resulting higher rates reduced the CO deviations from equilibrium. It is seen from Figure 2 that the CO deviations from equilibrium

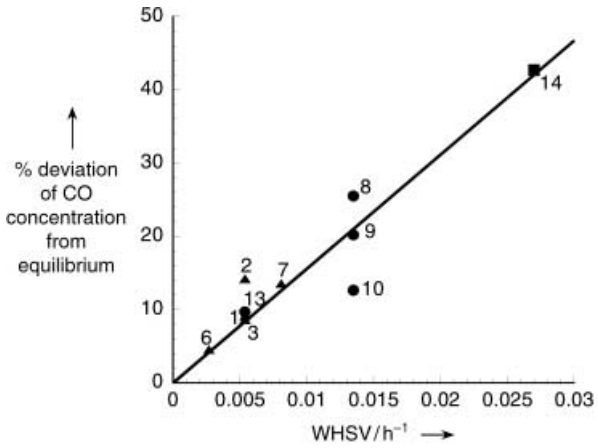

Figure 2. Effect of WHSV on the % deviation of CO concentration from equilibrium. The numbers alongside each point correspond to the run numbers (see Table 1). Triangles: 2% EG (runs 1–3, 6–7); Circles: 5% EG (runs 8–10, 13); and Squares: 10% EG (run 14).

increase with increasing space velocity, thus suggesting that these deviations may be caused by reaction kinetics effects involving the WGS reaction, such as adsorbed CO species react more rapidly with water to form CO_2 and H_2, compared to the slower desorption to form gaseous CO. Aupretre, et al.[12] have shown that H_2 and CO_2 were the primary gaseous products from steam reforming of ethanol, and CO was produced by the reverse WGS reaction.

Although the lowest levels of CO are obtained when the reactor is operated near the saturation pressure of water, this condition is not feasible for larger, nonvolatile feeds such as sorbitol and glucose, which undergo undesirable decomposition reactions when vaporized.[13] It thus becomes imperative to operate the reformer at system pressures above the saturation pressure of water to maintain liquid phase conditions. We now propose a new process, which we denote as ultra shift, to achieve very low levels of CO in the product gas from aqueous-phase reforming of oxygenated hydrocarbons, conducted at pressures above the saturation pressure of water. This process involves the vaporization of liquid water (in the shift zone) to dilute the H_2 and CO_2 in the bubbles, thereby favoring increased conversion of the WGS reaction and leading to lower CO concentrations.

Experiments were designed to demonstrate the feasibility of the ultra-shift process, and these data are included in Table 1. Reforming of a 2% EG feed, conducted at a system pressure of 32 bar with the shift-zone at 498 K (run 2), resulted in a CO concentration of 326 ppm. When the temperature of the shift zone was increased to 508 K (run 4), 91% of the water vaporized, thereby decreasing the H_2 pressure to 1.05 bar, and lowering the measured CO concentration to 84 ppm. In the case where the system pressure was 36.2 bar (runs 3 and 5), increasing the temperature of the shift zone from 498 to 515 K decreased the H_2 pressure from 7.53 to 1.14 bar and the measured CO concentration from 564 to 89 ppm. At the higher temperatures, the effect of diluting the H_2 and CO_2 pressures with water vapor supersedes the less favorable thermodynamics, leading to

ultra shift. Similar effects were observed for 5% EG, as seen in runs 9–12.

Figure 3a and 3b shows the effects of ultra shift on the levels of CO attained from reforming of 2 and 5% EG feeds. It is seen that when the shift temperature is maintained at the reforming temperature of 498 K, the effluent concentration of

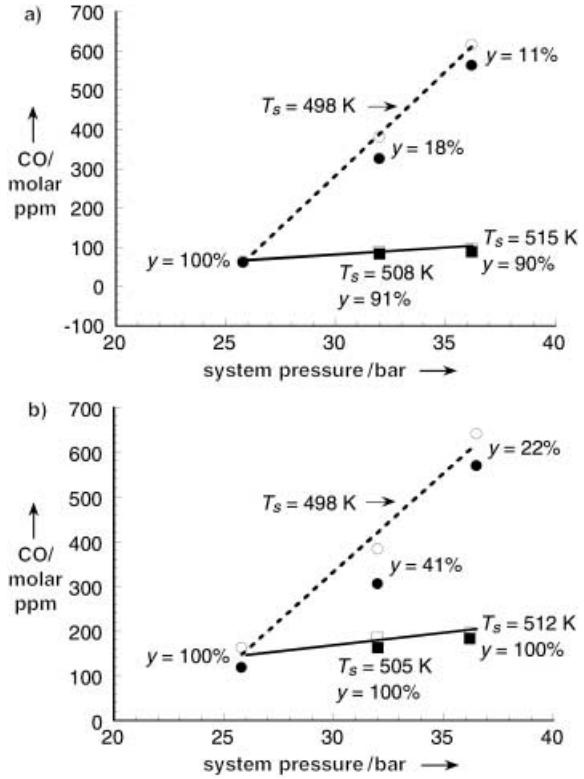

Figure 3. Effect of system variables on CO concentration for a) 2% EG (WHSV = 0.0054 h^{-1}) and b) 5% EG (WHSV = 0.0135 h^{-1}). Circles: CO concentration versus system pressure at shift temperature T_s = 498 K, Squares: Ultra shift at higher shift temperatures. Open symbols represent equilibrium CO and filled symbols represent observed CO.

CO increases as the system pressure is increased. When the shift temperature is increased such that a majority of the water vaporizes, then the product CO concentration, even at the higher pressures, decreases to below 100 ppm for 2% EG and below 200 ppm for 5% EG. Importantly, when the effluent from the reactor is subsequently cooled to a lower temperature to condense water, then the pressure of the noncondensable gases increases and approaches the system pressure. This process of ultra shift, involving initial vaporization followed by condensation of water, thus leads to the desirable production of fuel-cell-grade H_2 at high pressures and containing very low levels of CO.

Received: April 15, 2003 [Z51664]

Keywords: carbon monoxide · fuel cells · heterogeneous catalysis · hydrogen · water–gas shift

[1] M. Murthy, M. Esayian, W. Lee, J. W. Van Zee, *J. Electrochem. Soc.* **2003**, *150*, A29.
[2] J. Rostrup-Nielsen, *Phys. Chem. Chem. Phys.* **2001**, *3*, 283.
[3] H. Gunardson, *Industrial Gases in Petrochemical Processing*, Marcel Dekker, New York, **1998**.
[4] G. J. Grashoff, C. E. Pilkington, C. W. Corti, *Platinum Met. Rev.* **1983**, *27*, 157.
[5] P. G. Gray, M. I. Petch, *Platinum Met. Rev.* **2000**, *44*, 108.
[6] A. N. J. Van Keulen, in *US 6,207,307* USA, **2001**.
[7] C. S. Gittleman, R. Gupta, in *US 2002110503* USA, **2002**.
[8] R. D. Cortright, R. R. Davda, J. A. Dumesic, *Nature* **2002**, *418*, 964.
[9] R. R. Davda, J. W. Shabaker, G. W. Huber, R. D. Cortright, J. A. Dumesic, *Appl. Catal. B*, **2003**, *43*, 13.
[10] J. Novakova, L. Kubelkova, *Appl. Catal. B* **1997**, *14*, 273.
[11] J. W. Shabaker, R. R. Davda, G. W. Huber, R. D. Cortright, J. A. Dumesic, *J. Catal.*, **2002**, *215*, 344.
[12] F. Aupretre, C. Descorme, D. Duprez, *Catal. Commun.* **2002**, *3*, 263.
[13] B. M. Kabyemela, T. Adschiri, R. M. Malaluan, K. Arai, *Ind. Eng. Chem. Res.* **1999**, *38*, 2888.

